Hindawi
International Journal of Polymer Science
Volume 2020, Article ID 2785304, 9 pages
https://doi.org/10.1155/2020/2785304

Research Article

Effectual Anticancer Potentiality of Loaded Bee Venom onto Fungal Chitosan Nanoparticles

Adel I. Alalawy,[1] **Haddad A. El Rabey**,[1,2] **Fahad M. Almutairi**,[1] **Ahmed A. Tayel**,[3] **Mohammed A. Al-Duais**,[1,4] **Nahla S. Zidan**,[5,6] **and Mohamed I. Sakran**[1,7]

[1]*Biochemistry Department, Faculty of Science, University of Tabuk, Saudi Arabia*
[2]*Bioinformatics Department, Genetic Engineering and Biotechnology Research Institute, University of Sadat City, Sadat City, Egypt*
[3]*Faculty of Aquatic and Fisheries Sciences, Kafrelsheikh University, Egypt*
[4]*Chemistry Department, Faculty of Science, Ibb University, Yemen*
[5]*Department of Nutrition and Food Science, Faculty of Home Economics, University of Tabuk, Saudi Arabia*
[6]*Department of Home Economics, Faculty of Specific Education, Kafrelsheikh University, Egypt*
[7]*Biochemistry Section, Chemistry Department, Faculty of Science, Tanta University, Egypt*

Correspondence should be addressed to Haddad A. El Rabey; elrabey@hotmail.com
and Ahmed A. Tayel; tayel_ahmad@yahoo.com

Received 10 March 2020; Revised 12 April 2020; Accepted 17 April 2020; Published 23 May 2020

Guest Editor: Pooyan Makvandi

Chitosan and its nanoparticles (NPs) could be extracted from numerous fungal species and used as effectual carriers for bioactive compounds. The fungal chitosan (FC) was innovatively acquired from *Fusarium oxysporum* grown mycelia, characterized and used for NP synthesis and loading with bee venom (BV). The nano-FC (NFC) had 192.4 nm mean NP diameter, 38.22% loading capacity, and 92.42% entrapment efficiency. BV release from NFC was pH and time dependent; burst BV release was detected at the first 6 h, followed by gradual releases up to 30 h. The *in vitro* anticancer potentiality valuation, of NFC, BV, and NFC/BV nanoconjugates against HeLa cervix carcinoma, revealed that they all had potent dose-dependent anticancer activity; BV/NFC nanoconjugates were the most effective with $IC_{50} = 200\ \mu g/mL$. The fluorescent staining of treated HeLa cells with BV/NFC nanoconjugates, with DAPI and acridine orange/propidium iodide combination, indicated the appearance of early apoptosis, secondary apoptosis, and secondary necrosis markers and their increment with exposure prolongation. The production of NFC from *F. oxysporum* and their loading with BV are strongly counseled for production of potent natural antitumor agent with augmented activity against cervix carcinoma.

1. Introduction

Chitosan (Cts), the astounding amino polysaccharide derived from deacetylated chitin, has numerous practical advantages (e.g., its biodegradability, nontoxicity, biocompatibility, and effectual bioactivities) [1]. The Cts bioactivities encouraged its biomedical utilization in frequent applications (e.g., drug delivery, tissue engineering, anticancer treatment, antimicrobial formulations, and wound-healing dressing) [2]. The Cts charges and contents from amine groups are mostly the keys for its bioactive physiognomies (e.g., drug carrying, mucoadhesion, antimicrobial activity, drug release controlling, *in situ* gelation, and permeation enhancement) [3], which promoted its wide application as drug carrier and enhancer. Cts was promisingly extracted from the biomass of numerous fungal species [4–9]; the extracted fungal chitosan (FC) had comparable or superior bioactive attributes than accustomed commercial Cts.

Bee venom (BV) is the released defense weapon from honeybee (*Apis mellifera*) when their colony is attacked. BV

contains composited mixtures from bioactive peptides that could protect bees' colony against a broad diversity of predators and invaders. The contained bioactive components in BV include melittin (the major BV constituent), adolapin, apamin, degranulating peptide (for mast cell), enzymes (hyaluronidase and phospholipase A2), and some nonpeptide constituents (e.g., dopamine, histamine, and norepinephrine) [10, 11].

The BV or its constituents (e.g., melittin) were extensively investigated as potential treatment and inhibitors of tumor types; they exhibited multiple potential molecular anticancer mechanisms [11–13]. Numerous studies and reviews were documented to verify the anticancer capabilities of either BV or melittin toward various tumor types [14–18]; they concluded that BV with its components has auspicious anticancer and cytotoxic agents with broader spectrum toward multiple tumor cell types.

The nanotechnology involvement in most biomedical fields became much prevalent, including nanomaterial applications themselves as antimicrobial, anticancer, antiviral, and biocidal agents, or their loading with bioactive drugs/compounds to increase their solubility, stability, functionality, and delivery to the human body [19]. The nanopolymers, particularly nano-Cts and nano-FC (abbreviated thereafter as NFC), were from the most evaluated nanomaterials for their bioactivity and functionality as drug carriers, biopreservatives, and antimicrobial, anticancer, and gene delivery agents, individually or composited with other active compounds [3, 20–23].

The Cts nanoparticles were effectually used as carriers and enhancers of different animal venoms including snake, scorpion, and BV, for their evaluation as anticancer agents [24–28].

Accordingly, current study targeted the production of NFC, its loading with BV, and evaluation of their physiognomies and bioactivities to inhibit cervix adenocarcinoma (HeLa) cells and elucidate their potential action as anticancer agents.

2. Materials and Methods

2.1. Fungal Chitosan (FC) Extraction. Fungal culture, *Fusarium oxysporum* f. sp. *medicaginis*, ATCC® 52169™ (abbreviated thereafter as *Fom*), was used herein for FC production. Broth and agar media of potato dextrose (PDB and PDA, Difco Laboratories, Sparks, MD) were employed for *Fom* culture propagation and maintenance. Fungal incubation in PDB was prolonged for 7 days at 28°C under agitated aerobic conditions. The FC extraction was accomplished according to Tayel et al. [6]. Briefly, after cultivation, *Fom* mycelia were harvested via filtration, washed by deionized water (DW), and dried at 45°C in air oven. Dried *Fom* mycelia were deproteinized (using 1 M of NaOH), demineralized (using 1 M of acetic acid), and deacetylated (with 58% *w*/*v* NaOH solution at 110°C for 90 min); the filtration and extensive DW washing were repeated after each step. The FC deacetylation degree (DDA) was determined from its FTIR (Fourier-transform infrared spectroscopy) spectrum, using the Baxter et al. formula [29]:

$$\text{DDA}\,(\%) = 100 - \left(\frac{\text{A1655}}{\text{A3450}} \times 115\right), \quad (1)$$

whereas the FC molecular weight (MW) was measured via chromatography (gel permeation attached to refractive index detector (Postnova, Eresing, Germany)).

2.2. Synthesis of Nanofungal Chitosan Loaded with Bee Venom. The synthesis of nanoparticles (NPs) from FC and their loading with BV depended on previous method modifications [20, 24], using the incorporation technique. Briefly, stock solutions were made from FC (2.0 mg/mL, in diluted acetic acid solution), TPP (sodium tripolyphosphate, 1.0 mg/mL of DW), and BV (1.0 mg/mL of DW). The TPP solution was minutely dropped (at a rate of 350 μL/min) into vigorously stirred FC solution, up to a final ratio of FC : TPP = 3 : 1 *w*/*w*. The stirring continued for 60 min after TPP dropping, and the resulted illuminated suspension containing nanofungal chitosan (NFC) was centrifuged at 28.000 × *g*, washed with DW, recentrifuged, and lyophilized. For the BV-loaded NFC, the BV was firstly added to the FC solution (to have a BV concentration of 500 μg/mL), stirred for 30 min, then the TPP solution and the rest of the aforementioned steps were applied.

2.3. Characterization of Synthesized NPs

2.3.1. FTIR Spectrophotometry. The FTIR (PerkinElmer™ FTIR V. 10.03.08, Germany) spectra of FC, NFC, BV, and BV/NFC nanocomposite were measured at wavenumbers of 450-4000 cm^{-1}. Powdered samples were merged with KBr (at 1% ratio, *w*/*w*), and their FTIR transmission spectra were plotted.

2.3.2. NP Physiognomic Analysis. The NP size range, mean, median, distribution (polydispersity index (PDI)), and charges (zeta potential) were measured for NFC and BV/NFC nanoconjugates, using Zetasizer (Malvern Instruments, UK), based on DLS (dynamic light scattering) technique. Additionally, the shape, distribution, and size of synthesized BV/NFC nanoconjugates were screened via electron microscopy (Transmission) imaging (TEM, Leica™ Leo0430, Cambridge Ltd, UK); the TEM carbon-coated grid was charged with NP solution and 1% uranyl acetate, air dried, and loaded into TEM for examination.

2.4. Evaluation of BV Encapsulation and Release

2.4.1. Protein Assay. Based on the "Bradford method," a standardized assay kit for protein (Pierce™ Coomassie, Thermo Scientific-Pierce, Rockford, IL) was operated for determining free BV concentration in the NP solution. The formed color from BV conjugation was spectrophotometrically measured at 595 nm absorption. BSA (bovine serum albumin) was utilized as the comparable standard protein.

2.4.2. Loading and Encapsulation Efficiency Measurement. Specified amounts (10 μg) from BV-loaded NFC were

dissolved in DW in centrifugal tubes by vigorous vortexing, and then, the solution was centrifuged at $28.000 \times g$ for 35 min at 10°C. The BV loading capacity (LC) and encapsulation efficiency (EE) were calculated as follows [20]:

$$\text{LC}\,(\%) = \left(\frac{\text{Total BV amount} - \text{Free BV in supernatant}}{\text{NP weight}}\right) \times 100,$$
$$\text{EE}\,(\%) = \left(\frac{\text{Total BV amount} - \text{Free BV in supernatant}}{\text{Total BV amount}}\right) \times 100. \quad (2)$$

2.4.3. In Vitro BV Release. For BV release examination, the BV/NFC-NPs were transferred after centrifugation to clean centrifugal tubes with 3 mL of acetate buffer (pH 5.2) or phosphate buffer (PBS, pH 7.1). The tubes were maintained at 37 ± 1°C, and 100 μL samples were collected at time intervals of 2 h for 30 h; then, the protein contents were measured spectrophotometrically for each sample.

The released BV protein mass (M_i) at specific time (i) was calculated as follows [20]:

$$M_i = C_i V + \sum C_i - {}_1 V_s, \quad (3)$$

where C_i is the BV concentration in release solution at time i, V is the total release solution volume, and V_s is the sample volume.

2.5. NP Anticancer Activity

2.5.1. Cell Line Culture. Human cell lines of cervix carcinoma (HeLa) obtained from EGY-NCI (National Cancer Institute, Cairo, Egypt) were used. Culturing of HeLa cells in EMEM medium (supplemented with 10% (v/v) fetal calf serum, 2.0 mM L-glutamine, 0.1 mM nonessential amino acids, 1.5 g/L $NaHCO_3$, and 1.0 mM sodium pyruvate) was performed in humidified air with 5% CO_2 at 37°C.

2.5.2. Evaluation of NP Antiproliferative Activity. The BV/NFC-NPs antiproliferative activity was assessed using MTT (3-(4,5-dimethylthiazole-2-yl)-2,5-diphenyltetrazolium bromide) reduction assay [30]. In a 96-well polystyrene plate, each well contained 100 μL from complete medium, tumor cells ($\sim 1 \times 10^4$) were inoculated and incubated for 24 h in humidified air with 5% CO_2 at 37°C. After cell adherence, wells received gradual amounts of NFC, BV, and BV/NFC-NPs, after dissolving in DW, to have a concentration range of 0-500 μg/mL from each agent. After another 24 h of incubation, fresh media were added to replace the treatment solution and 10 μL of MTT solution (5 mg/mL of media without phenol red and serum) and plates were additionally incubated for further 3 h until purple formazan color appeared. After supernatant discarding, formazan crystals were dissolved with 100 μL of DMSO and the color was appraised at 540 nm absorbance within 1 h. Plain DMSO served as control.

The cell viability (%) was calculated as [(Absorbance of treated)/(Absorbance of control)] × 100.

2.5.3. Valuation of HeLa Cell Apoptosis Using Acridine Orange/Propidium Iodide Combined Staining. The HeLa cell potential apoptosis, after treatment with BV/NFC nanoconjugate, was valuated via combined staining with acridine orange (AO) and propidium iodide (PI) [31]. HeLa cell suspension ($\sim 2 \times 10^5$ cells/mL) was treated with BV/NFC-NPs at 500 μg/mL concentration and incubated for 24 and 48 h in humidified air with 5% CO_2 at 37°C. Treated and control cells were rinsed using PBS, then double stained for 15 min with AO (10 mg/mL) and PI (4 mg/mL) in the dark. Images were captured (using fluorescence microscope Olympus BX51, Tokyo, Japan) based on the appearance of apoptosis indicators, i.e., the green-, orange-, and red-stained cells/organelles, within 25 min after staining.

2.5.4. Appraisal of Cell Apoptosis via DAPI Staining. The BV/NFC-NPs-induced apoptosis was further analyzed using nuclear dye DAPI (4′,6-diamidino-2-phenylindole) fluorescent staining to detect nucleic DNA fragmentation and condensation in treated cells [32]. The treated HeLa cells were handled as mentioned in Section 2.5.3; then, after PBS washing, they were fixed with paraformaldehyde (4%) for 12 min and permeabilized with buffer (containing 0.5% Triton X-100 and 3% paraformaldehyde), then 50 μL of DAPI (with 1 μg/mL concentration) was added and kept for 60 min. The fluorescent micrographs were captured to demonstrate the liberated and condensed nuclei fragments stained by DAPI fluorescent dye.

3. Results

The FC extraction and production, from *Fom* grown mycelia, were gainfully achieved in this work; the FC productivity was 2.41 g/L of fermentation medium. The produced FC had a molecular weight of 51.6 kDa and DDA of 88.4%.

The process effectiveness of ionic gelation to transform FC into NFC and loading it with BV was assessed using FTIR to reveal their biochemical bonding and interactions.

The FTIR spectra of FC, NFC, BV, and NFC/BV nanoconjugates are presented in Figure 1. In the spectrum of *Fom*-extracted FC (Figure 1, FC), the strong peak around 3452 cm^{-1} corresponds to the combined hydrogen bonding and O–H stretching; the N–H stretching (from primary amines) was overlapped in this region. The specified absorption peaks and bands of the FC were detected at 1718 cm^{-1} (carbonyl (C=O) stretching of the secondary amide I band), peaks at 1539 cm^{-1} and 1324 cm^{-1} (designated the amide II (N–H) bending vibration and the absorption of amide III, respectively), and at 1079 cm^{-1} (belongs to the C–O–C stretching). The spectrum of NFC (Figure 1, NFC) indicated some differences from FC spectrum; the peak of 3452 cm^{-1} in FC became wider in NFC with amplified relative intensity, which indicates the enhancement in hydrogen bonding. The NFC spectrum showed also a sharp P=O peak at 1174 cm–1, indicating the cross-linkage with TPP. Generally, the main characteristic peaks and bands in FC spectrum appeared in NFC spectrum, but with slight shifting of them to close wavenumbers.

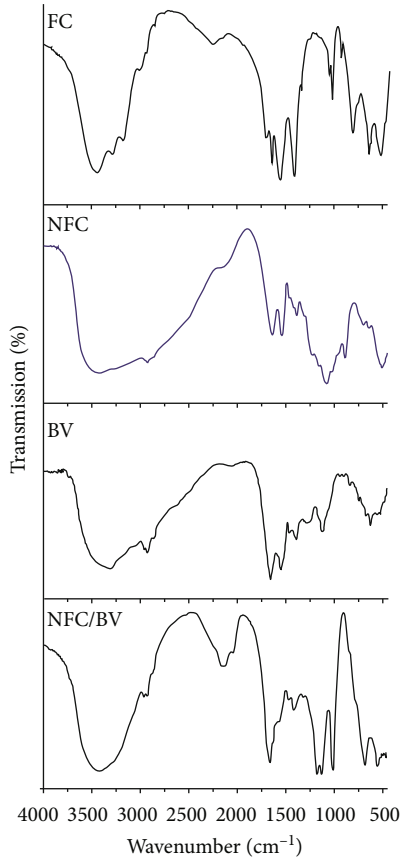

Figure 1: FTIR spectra of synthesized molecules of fungal chitosan (FC), bee venom (BV), nano-FC (NFC), and BV/NFC nanocomposite.

For the BV spectrum, the observed peak at absorbance region of 3250–3450 cm^{-1} indicates the free vibrations of N–H stretching. The FTIR spectrum of BV also indicated the characteristic amide bands, i.e., amide I (1651 cm^{-1}), amide II (1532 cm^{-1}), and the bands at 1112 cm^{-1} and 1040 cm^{-1} that indicate unsystematic coil conformation (Figure 1, BV). In the FTIR spectrum of NFC/BV nanoconjugate, the BV absorbance peak for N–H stretching at 3318 cm^{-1} was reduced and shifted to 3421 cm^{-1} (Figure 1, NFC/BV). The amide I indicated band in the BV at 1651 cm^{-1} was also shifted to a higher wavenumber (1654 cm^{-1}) in BV/NFC.

The characteristic attributes of synthesized NP from FC and BV are illustrated in Table 1.

The NFC had smaller average (mean) particle diameters, median diameter, and size range than BV/NFC nanocomposite. The PDI values were <0.5 for both synthesized NPs (0.262 for NFC and 0.414 for BV/NFC nanocomposite), which indicates a matched and favorable NP size distribution (Table 1). Both NP types had positive Z-potentialities; the BV loading into NFC slightly reduced their positivity from +33.7 (for NFC) to +27.2 (for BV/NFC nanocomposite).

The particle shape, size, and distribution, for BV/NFC nanocomposite, were further elucidated via TEM imaging (Figure 2). The nanoconjugate particles mostly appeared with spherical shapes and smooth surfaces, uniform distribution with size range of ~168-256 nm (Figure 2).

The calculated LC and EE, of BV in NFC, were 38.22 and 92.42%, respectively. The BV release from NFC was *in vitro* evaluated at pH 5.2 and 7.0, through direct dispersion during 30 h of release duration. The BV release patterns from NFC are plotted in Figure 3.

The BV release had a pH- and time-dependent manner; lower BV percentages were released in pH 7.1 than in pH 5.2. The releasing pattern revealed a burst BV release at the first 6 h; after that, gradual releases were detected with experiment prolongation for 30 h. The released BV ratios were 67.2 and 71.4% after 6 h, and the maximum release percentages were 76.2 and 81.3%, at the duration end, in pH 7.1 and5.2, respectively.

The anticancer potentialities of NFC, BV, and FC/BV-NPs measured with the decrement of HeLa cell viability, after exposure to different concentrations from synthesized agents, are plotted in Figure 4. The entire agents had potent anticancer activity toward examined cells; the activities of all agents were dose-dependent. The most forceful agent was the NFC/BV nanoconjugates then the BV and lastly the NFC. After 24 h of exposure to a concentration of 500 μg/mL, only 8.3 and 22.3% of cells remained viable after treatment with NFC/BV-NPs and BV, respectively. The 200 μg/mL concentration from NFC/BV-NPs could kill 50% of cancerous cells after 24 h (Figure 4).

Fluorescent imaging was applied to elucidate the cytotoxic effects of NFC/BV composites toward examined cancerous cells (Figure 5). The potential apoptotic effect after HeLa cell treatment with NFC/BV nanoconjugates (at 500 μg/mL concentration) was investigated using DAPI staining (Figure 5, DAPI). The exposure to nanoconjugate induced observable morphological apoptosis signs in treated HeLa cells, e.g., membrane blebbing, cell shrinkage and rounding.

The apoptosis signs greatly increased and became more vigorous, with exposure prolongation from 24 to 48 h, to include most of the treated cancerous cells. While control cells had no apoptosis signs, the DAPI-stained treated cells had many brightly fluoresced fragments/nuclei; the DNA condensation and apoptosis signs increased dramatically in a time-dependent approach.

The cell apoptosis and necrosis were further elucidated via AO/PI double fluorescent staining (Figure 5, AO/PI); viable cancerous cells appeared with intact structures and green color for cells and nuclei. The early apoptosis signs include the appearance of chromatin condensation and bright green-stained nuclei, which clearly appeared after 24 h from treatment with NFC/BV nanoconjugate. The secondary necrosis and late apoptosis signs evidently appeared in HeLa cells after treatment for 48 h, with more chromatin condensation, dense orange-stained areas, and many stained nuclei with deep reddish-orange color.

4. Discussion

The achievement of FC was successfully conducted from *Fom* mycelia, which confirmed the investigations that indicated the high potentiality of fungi as sustainable sources for

Table 1: Characteristic attributes of synthesized nanoparticles from fungal chitosan (NFC) and its nanocomposite with bee venom (BV/NFC).

Nanoparticles	Size range (nm)	Median diameter (nm)	Mean diameter (nm)	Z-potential (mV)	PDI
NFC	92.1-157.3	121.6	129.1	+33.7	0.262
BV/NFC nanocomposite	147.3-269.6	186.3	192.4	+27.2	0.414

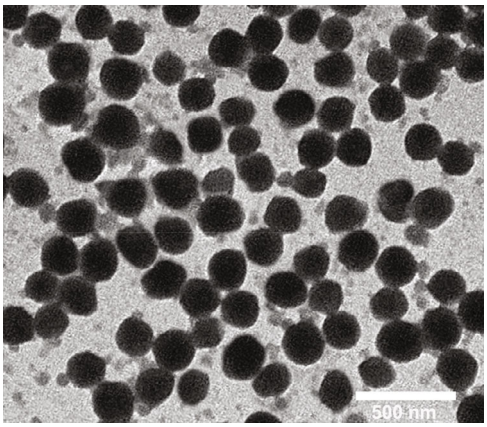

Figure 2: Transmission micrographs of synthesized nanocomposite from fungal chitosan and bee venom.

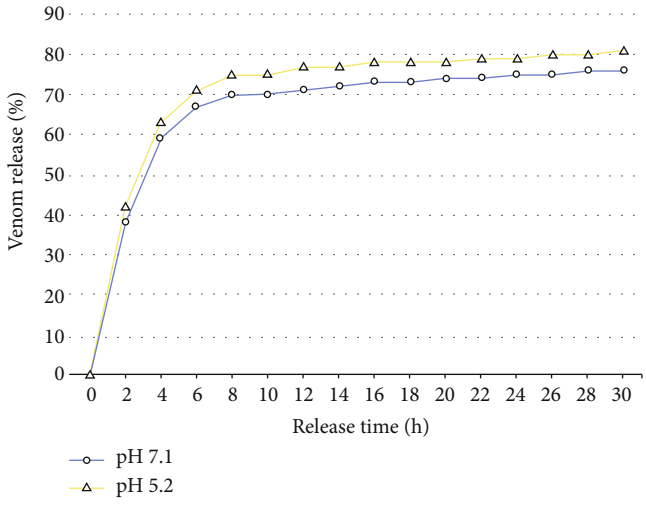

Figure 3: Bee venom release profile from fungal chitosan nanoparticles at different pH values (5.2 and 7.1) during the 30 h releasing period.

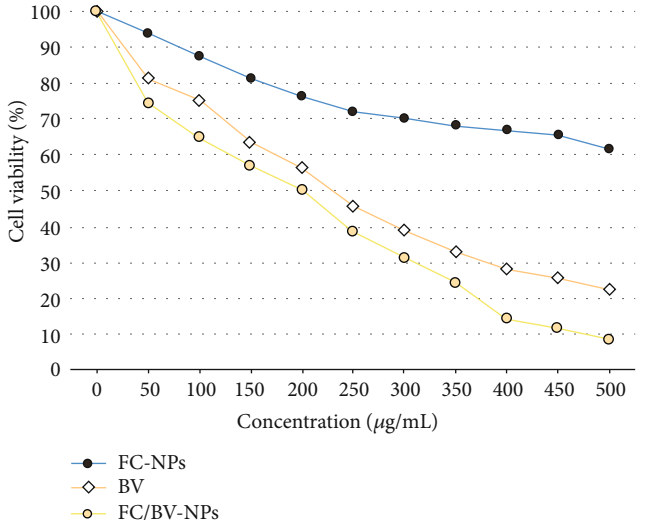

Figure 4: Cancer cell (HeLa) viability after exposure to nanofungal chitosan (FC-NPs), bee venom (BV), and their nanocomposite (FC/BV-NPs) for 24 h using different concentrations from each of them.

chitosan production [4–9, 22, 23]; these investigations recommended the application of FC, from many fungal species, in the biomedical and health-related fields.

The FTIR analysis of FC certified its comparable structure/groups to the standardized conventional chitosan [6, 33].

The slight shifting of many characteristic peaks and bands in FC spectrum to close wavenumbers in NFC spectrum validates the successful NFC cross-linkage and synthesis of targeted NPs [22]. The NFC and NFC/BV spectra were closely matched in most of the biochemical groups and wavenumber intensity; this indicates that BV did not chemically affect or change the NFC structure and accordingly maintain its biosafety for usage in the human body [29]. In the FTIR spectrum of NFC/BV nanoconjugate, the stretching and broadening of C–O (from NFC) and reduction of stretched N–H intensity (from BV) and their shifting to littler wavenumbers indicate the hydrogen bond formation between these active groups from BV and NFC [34].

The obtained data from "Zetasizer," regarding the synthesized NFC and BV/NFC nanoconjugate, revealed that BV/NFC nanoparticles had larger sizes than NFC particles; this could conceivably be due to the added molecular weight and composited structure after venom on nanochitosan [27], which verifies the elevated ability of current NFC to carry BV. For successful biomedical applications, functional nanocomposites are mostly manufactured in a NP size range from 20 up to 300 nm, considering that the "smallest particles could reach any part of the body" [35].

The BV release from NFC was very fast in the first 6 h of the experiment; this burst release is supposed to depend on the BV dissociation from the surface of NFC, as generally reported from loaded protein molecules on nanochitosan [21, 36]. Additionally, the early rapid release and diffusion of protein molecules from the surface of nanoparticles were stated as undeniable [37]. Subsequently, the slow BV release was seemingly attributed to slow degradation of entrapped protein molecules in NFC and the degradation of

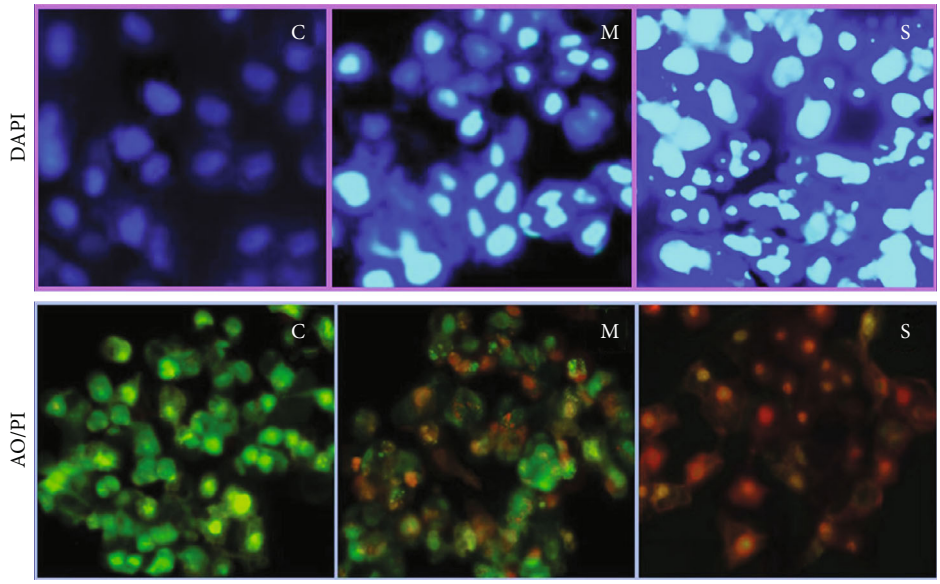

Figure 5: Fluorescent microscopic imaging of HeLa cancerous cells, stained with DAPI stain or acridine orange/propidium iodide (AO/PI) double staining, after treatment with 500 μg/mL from bee venom/fungal chitosan nanoparticles*. *C: control (untreated) cells; M: treated cells for 24 h; S: treated cells for 48 h.

nanoparticles itself [38]. The degradation rate of protein was supposed to exceed its releasing rate, after prolonged releasing period [39]. Additionally, BV was reported to engage the long chain of nanochitosan in a nonuniform manner, thus high percentages from it could be easily released in the early releasing period [28].

The release of BV was higher in pH 5.2 than in pH 7.1, which could be explained by the solubility preference of chitosan in weak acidic solutions than in neutral solutions; thus, the pH 5.2 condition could increase BV liberating from the solubilized NFC.

The induction of HeLa cell apoptosis/necrosis, after treatment with BV/NFC nanoconjugate, was evidenced via staining with fluorescent dyes. The lethal effect of BV/NFC nanoconjugates could be principally owed to BV anticancer potentiality, which was strengthened after loading onto NFC. The NFC polycationic nature is suggesting for facilitating particle attachment to tumor cells and enables more contact between BV and cell surface.

Animal venom peptides, especially BV, have a great potential for developing into biopharmaceuticals, with many limitations that could be overcome with their conjugation with polymeric nanocarriers like Cts to augment their chemical instability, half-lives, oral absorption, and target cytotoxicity [40].

Although the produced bioactive agents (NFC and BV) were extracted from fungal and insect sources, the transability of other biological components from these organisms to the human body is not expected because Cts and NFC are mostly polysaccharides extracted with harsh steps (e.g., very high alkalinity and temperature), leading to the elimination of any protein residues, while the BV is obtained from the bees' toxin glands and is anciently applied for treating various diseases with no evidences for genetic transferability during these treatments [13]. Nanoformulations are demonstrated as well-suited for the administration of drug-like molecules; polymeric nanocarriers can enhance the drugs' half-life circulation and their deposition into diseased sites with diminished extravasation to healthy/normal tissues [41].

The BV antitumor activity was stated to depend primarily on close contact between its active constituents and cancer cells, which is essential to develop cell apoptosis/necrosis [42]. Melittin (the major protein constituent of BV) was confirmed for cancer therapy as a potent bioactive agent [43]; the main suggested functions of melittin involved cell membrane perturbing (leading to hemolytic and antimicrobial consequences) and the induction of vigorous structural alterations in these membranes (including pore formation, vesiculation, and fusion) [44]. Furthermore, melittin was verified to induce arrest in tumor cell cycle, inhibiting their growth, and apoptosis signs in different tumor cells [12]. Interestingly, BV melittin was demonstrated to specifically pursue cells that have extraordinary levels from Ras oncogene, i.e., tumor cells [45].

Apoptosis was appointed as the key function of BV anticancer action, as consequences from death receptor (DR) stimulation and inactivation of nuclear growth factor family kappa B (NF-κB) in cancer cell [11].

The application of AO/PI double fluorescent staining, for quantifying the apoptotic and necrotic consequence of BV/NFC nanoconjugate on HeLa cells, proved its applicability and efficiency. The variations in cell staining with green, orange, and reddish-orange as indicators for early apoptosis, late apoptosis, and secondary necrosis, respectively, were illustrated [31]. The tumor cell death indicators (apoptosis, necrosis, and lysis) were stated as the potential mechanisms, by which BV could inhibit tumor development [17]. A previous study [46] indicated that BV anticancer activity was more forceful against V79 than for HeLa cells; and its effect toward both cells was dose-dependent. The BV

role in the *in vivo* inhibition of cancer growth and proliferation was addressed to involve immune response stimulation of lymph nodes [42].

Interestingly, BV was illustrated to induce leukemia cell apoptosis, with no cytotoxicity on normal cells of the bone marrow [15]; the main regulators of BV-induced leukemic cell apoptosis are caspase-3 and Bcl-2 via suppression of mitogen-activated signaling paths [14]. The preceding flow cytometric analysis indicated BV capability for inducing ROS (reactive oxygen species) production, increasing cytoplasmic Ca^{2+} levels, releasing cytochrome C due to reduced potentials of mitochondrial membrane, and promoting caspase-3 activation, which consequently caused cell apoptosis [16].

The amount of BV binding sites from carbohydrate/amines on cancerous cell membranes was suggested to explain the varying sensitivity of cancer types to BV components [46]; thus, it is supposable here that loaded NFC with BV could generate more binding sites with HeLa cell membranes and accordingly strengthen the BV antiproliferative action toward these cells.

The modern approaches for NP safety assessment recommended the usage of in vitro/ex vivo models as essential prerequisites for their translation into applicable products [47]. The Safe-by-Design (SbD) concept is applied for the assessment of nanomaterial and nanopolymer potential consequences on the environment and human health and their uses to develop nanomedicines; according to the latest SbD criteria, NFC could be regarded as an ideal safe "nanobiocarrier" for delivering BV into the human body to fight cancer cells [48, 49].

5. Conclusion

The grown mycelia of *Fom* were innovatively employed as FC source, which was successfully utilized for NFC production and loading with BV. The BV/NFC nanoconjugate had favorable structural and biochemical physiognomies, plus their augmented anticancer bioactivity against cervix carcinoma (HeLa) cells. The BV/NFC nanoconjugate could induce serious apoptosis signs in HeLa cells in a time- and dose-dependent manner. The application and extra evaluation of BV/NFC nanoconjugates are strongly recommended as effective and natural anticancer agents.

Data Availability

The datasets generated during and/or analyzed during the current study are available from the corresponding author on reasonable request.

Conflicts of Interest

The authors declare that they have no conflicts of interest.

Acknowledgments

This work was supported from the "Deanship of Scientific Research, University of Tabuk, KSA," under the Research Group (no. RGP-S-1440-0133).

References

[1] E. I. Rabea, M. E. Badawy, C. V. Stevens, G. Smagghe, and W. Steurbaut, "Chitosan as antimicrobial agent: applications and mode of action," *Biomacromolecules*, vol. 4, no. 6, pp. 1457–1465, 2003.

[2] O. Felt, P. Buri, and R. Gurny, "Chitosan: a unique polysaccharide for drug delivery," *Drug Development and Industrial Pharmacy*, vol. 24, no. 11, pp. 979–993, 1998.

[3] A. Ali and S. Ahmed, "A review on chitosan and its nanocomposites in drug delivery," *International Journal of Biological Macromolecules*, vol. 109, pp. 273–286, 2018.

[4] A. A. Tayel, S. Moussa, K. Opwis, D. Knittel, E. Schollmeyer, and A. Nickisch-Hartfiel, "Inhibition of microbial pathogens by fungal chitosan," *International Journal of Biological Macromolecules*, vol. 47, no. 1, pp. 10–14, 2010.

[5] S. H. Moussa, A. A. Tayel, and A. I. Al-Turki, "Evaluation of fungal chitosan as a biocontrol and antibacterial agent using fluorescence-labeling," *International Journal of Biological Macromolecules*, vol. 54, pp. 204–208, 2013.

[6] A. A. Tayel, S. I. A. Ibrahim, M. A. al-Saman, and S. H. Moussa, "Production of fungal chitosan from date wastes and its application as a biopreservative for minced meat," *International Journal of Biological Macromolecules*, vol. 69, pp. 471–475, 2014.

[7] A. A. Tayel, M. M. Gharieb, H. R. Zaki, and N. M. Elguindy, "Bio-clarification of water from heavy metals and microbial effluence using fungal chitosan," *International Journal of Biological Macromolecules*, vol. 83, pp. 277–281, 2016.

[8] A. A. Tayel, "Microbial chitosan as a biopreservative for fish sausages," *International Journal of Biological Macromolecules*, vol. 93, article Part A, pp. 41–46, 2016.

[9] M. S. Alsaggaf, S. H. Moussa, N. M. Elguindy, and A. A. Tayel, "Fungal chitosan and *Lycium barbarum* extract as anti-listeria and quality preservatives in minced catfish," *International Journal of Biological Macromolecules*, vol. 104, article Part A, pp. 854–861, 2017.

[10] H. Raghuraman and A. Chattopadhyay, "Melittin: a membrane-active peptide with diverse functions," *Bioscience Reports*, vol. 27, no. 4-5, pp. 189–223, 2007.

[11] S. C. Pak, "Health benefits and uses in medicine of bee venom," in *Bee Products - Chemical and Biological Properties*, J. M. Alvarez-Suarez, Ed., pp. 287–306, Springer Int. Pub. AG, Cham, Switzerland, 2017.

[12] N. Oršolić, L. Šver, K. Bendelja, and I. Bašić, "Antitumor activity of bee venom," *Periodicum Biologorum*, vol. 103, pp. 49–54, 2001.

[13] A. Aufschnaiter, V. Kohler, S. Khalifa et al., "Apitoxin and its components against cancer, neurodegeneration and rheumatoid arthritis: limitations and possibilities," *Toxins*, vol. 12, no. 2, p. 66, 2020.

[14] S. J. Hong, G. S. Rim, H. I. Yang et al., "Bee venom induces apoptosis through caspase-3 activation in synovial fibroblasts of patients with rheumatoid arthritis," *Toxicon*, vol. 46, no. 1, pp. 39–45, 2005.

[15] D. O. Moon, S. Y. Park, M. S. Heo et al., "Key regulators in bee venom-induced apoptosis are Bcl-2 and caspase-3 in human leukemic U937 cells through downregulation of ERK and Akt," *International Immunopharmacology*, vol. 6, no. 12, pp. 1796–1807, 2006.

[16] S. W. Ip, H. C. Wei, J. P. Lin et al., "Bee venom induced cell cycle arrest and apoptosis in human cervical epidermoid

carcinoma Ca Ski cells," *Anticancer Research*, vol. 28, no. 2A, pp. 833–842, 2008.

[17] N. Oršolić, "Bee venom in cancer therapy," *Cancer Metastasis Reviews*, vol. 31, no. 1-2, pp. 173–194, 2012.

[18] G. Gajski and V. Garaj-Vrhovac, "Melittin: a lytic peptide with anticancer properties," *Environmental Toxicology and Pharmacology*, vol. 36, no. 2, pp. 697–705, 2013.

[19] S. K. Sahoo, S. Parveen, and J. J. Panda, "The present and future of nanotechnology in human health care," *Nanomedicine: Nanotechnology, Biology and Medicine*, vol. 3, no. 1, pp. 20–31, 2007.

[20] Q. Gan and T. Wang, "Chitosan nanoparticle as protein delivery carrier—systematic examination of fabrication conditions for efficient loading and release," *Colloids and Surfaces B: Biointerfaces*, vol. 59, no. 1, pp. 24–34, 2007.

[21] S. Jarudilokkul, A. Tongthammachat, and V. Boonamnuayvittaya, "Preparation of chitosan nanoparticles for encapsulation and release of protein," *Korean Journal of Chemical Engineering*, vol. 28, no. 5, pp. 1247–1251, 2011.

[22] S. Alsharari, A. A. Tayel, and S. H. Moussa, "Soil emendation with nano-fungal chitosan for heavy metals biosorption," *International Journal of Biological Macromolecules*, vol. 118, article Part B, pp. 2265–2268, 2018.

[23] H. A. El Rabey, F. M. Almutairi, A. I. Alalawy et al., "Augmented control of drug-resistant *Candida* spp. via fluconazole loading into fungal chitosan nanoparticles," *International Journal of Biological Macromolecules*, vol. 141, pp. 511–516, 2019.

[24] N. M. Dounighi, M. Damavandi, H. Zolfagharian, and S. Moradi, "Preparing and characterizing chitosan nanoparticles containing *Hemiscorpius lepturus* scorpion venom as an antigen delivery system," *Archives of Razi Institute*, vol. 67, pp. 145–153, 2012.

[25] N. Dounighi, M. Mehrabi, M. R. Avadi, H. Zolfagharian, and M. Rezayat, "Preparation, characterization and stability investigation of chitosan nanoparticles loaded with the *Echis carinatus* snake venom as a novel delivery system," *Archives of Razi Institute*, vol. 70, pp. 269–277, 2015.

[26] N. Mohammadpour Dounighi, R. Eskandari, M. R. Avadi, H. Zolfagharian, A. Mir Mohammad Sadeghi, and M. Rezayat, "Preparation and in vitro characterization of chitosan nanoparticles containing *Mesobuthus eupeus* scorpion venom as an antigen delivery system," *Journal of Venomous Animals and Toxins including Tropical Diseases*, vol. 18, no. 1, pp. 44–52, 2012.

[27] K. S. Rocha Soares, J. L. Cardozo Fonseca, M. A. Oliveira Bitencourt, K. S. C. R. Santos, A. A. Silva-Júnior, and M. F. Fernandes-Pedrosa, "Serum production against *Tityus serrulatus* scorpion venom using cross-linked chitosan nanoparticles as immunoadjuvant," *Toxicon*, vol. 60, no. 8, pp. 1349–1354, 2012.

[28] F. A. Taher, W. A. Moselhy, A. F. Mohamed, S. E. Didamony, K. M. Metwalley, and A. B. Zayed, "Preparation and characterization of shrimp derived chitosan and evaluation of its efficiency as bee venom delivery for cancer treatment," *International Journal of Advanced Research*, vol. 5, no. 5, pp. 370–388, 2017.

[29] A. Baxter, M. Dillon, K. D. Anthony Taylor, and G. A. F. Roberts, "Improved method for I.R. determination of the degree of N-acetylation of chitosan," *International Journal of Biological Macromolecules*, vol. 14, no. 3, pp. 166–169, 1992.

[30] D. Chowrasia, C. Karthikeyan, L. Choure et al., "Synthesis, characterization and anti cancer activity of some fluorinated 3,6-diaryl-[1,2,4]triazolo[3,4-b][1,3,4]thiadiazoles," *Arabian Journal of Chemistry*, vol. 10, pp. S2424–S2428, 2017.

[31] M. Hajrezaie, M. Paydar, C. Y. Looi et al., "Apoptotic effect of novel Schiff based $CdCl_2(C_{14}H_{21}N_3O_2)$ complex is mediated via activation of the mitochondrial pathway in colon cancer cells," *Scientific Reports*, vol. 5, no. 1, article 9097, 2015.

[32] M. A. Rahman and A. Hussain, "Anticancer activity and apoptosis inducing effect of methanolic extract of *Cordia dichotoma* against human cancer cell line," *Bangladesh Journal of Pharmacology*, vol. 10, no. 1, pp. 27–34, 2015.

[33] A. A. Tayel, S. H. Moussa, W. F. El-Tras, N. M. Elguindy, and K. Opwis, "Antimicrobial textile treated with chitosan from *Aspergillus niger* mycelial waste," *International Journal of Biological Macromolecules*, vol. 49, no. 2, pp. 241–245, 2011.

[34] M. Qiao, D. Chen, T. Hao, X. Zhao, H. Hu, and X. Ma, "Effect of bee venom peptide-copolymer interactions on thermosensitive hydrogel delivery systems," *International Journal of Pharmaceutics*, vol. 345, no. 1-2, pp. 116–124, 2007.

[35] H. F. Krug and P. Wick, "Nanotoxicology: an interdisciplinary challenge," *Angewandte Chemie (International Ed. in English)*, vol. 50, no. 6, pp. 1260–1278, 2011.

[36] Q. Gan, T. Wang, C. Cochrane, and P. McCarron, "Modulation of surface charge, particle size and morphological properties of chitosan–TPP nanoparticles intended for gene delivery," *Colloids and Surfaces B: Biointerfaces*, vol. 44, no. 2-3, pp. 65–73, 2005.

[37] S. Zhou, X. Deng, and X. Li, "Investigation on a novel core-coated microspheres protein delivery system," *Journal of Controlled Release*, vol. 75, no. 1-2, pp. 27–36, 2001.

[38] S. Zhou, X. Deng, M. Yuan, and X. Li, "Investigation on preparation and protein release of biodegradable polymer microspheres as drug-delivery system," *Journal of Applied Polymer Science*, vol. 84, no. 4, pp. 778–784, 2002.

[39] M. Amidi, S. G. Romeijn, G. Borchard, H. E. Junginger, W. E. Hennink, and W. Jiskoot, "Preparation and characterization of protein-loaded N-trimethyl chitosan nanoparticles as nasal delivery system," *Journal of Controlled Release*, vol. 111, no. 1-2, pp. 107–116, 2006.

[40] A. P. dos Santos, T. G. de Araújo, and G. Rádis-Baptista, "Nanoparticles functionalized with venom-derived peptides and toxins for pharmaceutical applications," *Current Pharmaceutical Biotechnology*, vol. 21, no. 2, pp. 97–109, 2020.

[41] S. Bisso and J. C. Leroux, "Nanopharmaceuticals: a focus on their clinical translatability," *International Journal of Pharmaceutics*, vol. 578, article 119098, 2020.

[42] N. Oršolić, L. Sver, S. Verstovsek, S. Terzic, and I. Basic, "Inhibition of mammary carcinoma cell proliferation in vitro and tumor growth in vivo by bee venom," *Toxicon*, vol. 41, no. 7, pp. 861–870, 2003.

[43] C. E. Dempsey, "The actions of melittin on membranes," *Biochimica et Biophysica Acta*, vol. 1031, no. 2, pp. 143–161, 1990.

[44] C. Leuschner and W. Hansel, "Membrane disrupting lytic peptides for cancer treatments," *Current Pharmaceutical Design*, vol. 10, no. 19, pp. 2299–2310, 2004.

[45] S. V. Sharma, "Melittin resistance: a counterselection for ras transformation," *Oncogene*, vol. 7, no. 2, pp. 193–201, 1992.

[46] N. Oršolić, "Potentiation of bleomycin lethality in HeLa and V79 cells by bee venom," *Archives of Industrial Hygiene and Toxicology*, vol. 60, no. 3, pp. 317–326, 2009.

[47] P. Wick, S. Chortarea, O. T. Guenat et al., "In vitro-ex vivo model systems for nanosafety assessment," *European Journal of Nanomedicine*, vol. 7, no. 3, pp. 169–179, 2015.

[48] S. Jesus, M. Schmutz, C. Som, G. Borchard, P. Wick, and O. Borges, "Hazard assessment of polymeric nanobiomaterials for drug delivery: what can we learn from literature so far," *Frontiers in Bioengineering and Biotechnology*, vol. 7, p. 261, 2019.

[49] M. Schmutz, O. Borges, S. Jesus et al., "A methodological safe-by-design approach for the development of nanomedicines," *Frontiers in Bioengineering and Biotechnology*, vol. 8, p. 258, 2020.